

## A FAULT DIAGNOSIS METHOD FOR SUBSTATION GROUNDING GRID BASED ON THE SQUARE-WAVE FREQUENCY DOMAIN MODEL

Peng-He Zhang<sup>1)</sup>, Jun-Jia He<sup>1)</sup>, Dan-Dan Zhang<sup>1)</sup>, Lan-Min Wu<sup>2)</sup>

1) College of Electrical and Electronic Engineering, Huazhong University of Science and Technology, Wuhan, China  
(✉ zzpvh2004@126.com, +86 13871123500)

2) Shan Xi Province Electrical Power Company, Taiyuan 03000, ShanXi Province (389619845@qq.com)

### Abstract

Current methods of fault diagnosis for the grounding grid using DC or AC are limited in accuracy and cannot be used to identify the locations of the faults. In this study, a new method of fault diagnosis for substation grounding grids is proposed using a square-wave. A frequency model of the grounding system is constructed by analyzing the frequency characteristics of the soil and the grounding conductors into which two different frequency square-wave sources are injected. By analyzing and comparing the corresponding information of the surface potentials of the output signals, the faults of the grounding grid can be diagnosed and located. Our method is verified by software simulation, scale model experiments and field experiments.

Keywords: square-wave, frequency characteristics, grounding grid, fault diagnosis.

© 2012 Polish Academy of Sciences. All rights reserved

### 1. Introduction

Grounding is the most important approach to guaranteeing the safety of a power system. But it is hard to monitor the state of a grounding grid, as it is usually buried under earth. Grid faults are also very likely to take place due to the corrosion of the earth electrodes. Some studies put forward the port nodal resistance (or voltage) method [1, 2] and the simple surface potentials method to diagnose a grid fault [3, 4] based on a time-domain characteristic analysis. The accuracy of such approaches is unsatisfactory because the change in port nodal resistance or voltage is too small. Greev and Dawalibi [5] built a model of the simple frequency characteristic of the grounding grid. Others have studied the frequency model of the grounding grid according to the complex image method [6-8]. Based on the frequency model, some diagnosed the broken location of a grounding grid by measuring the magnetic field on the ground [9, 10]. This approach has demonstrated improvement in accuracy in fault diagnosis; but during the process of measurement, due to the inevitable interference from the metal equipment and electromagnetic field, it is difficult to locate the fault of the grounding grid.

The diagnostic method based on the frequency domain has been used extensively in various fields, e.g. the transient electromagnetic method to detect the fault of a buried metal pipe [11], the electrochemical impedance spectrum method to monitor the corrosion of reinforced concrete [12], the earth electromagnetic method of geophysics to search for metal ore [13], the square-wave method of double frequencies to detect metal [14], etc.

In this paper, a fault diagnosis method for the grounding system is proposed based on the frequency domain. Through analyzing the different frequency characteristics of metal and soil, the diagnostic method of square-wave frequency domain is presented. This method is

verified by conducting software simulation, scale model experiments and field experiments. The results demonstrate that this method can be used to successfully diagnose a fault of the grounding grid and identify the fault location.

## 2. Frequency domain characteristic of a grounding system

### 2.1. Frequency domain model of a grounding grid

The buried depth of a grounding grid is generally no more than 5 m; even in an area of high resistivity, the depth of vertical grounding conductors laid by the blast of a deep well is less than 80 m. According to the wave physics equation, the wave propagation speed is directly proportional to the wavelength and frequency:

$$v = \lambda f, \quad (1)$$

where:  $v$  is the wave propagation speed (determined by the dielectric constant and permeability), m/s;  $f$  is the frequency (determined by power), Hz;  $\lambda$  is the wavelength, m. When the frequency of the electromagnetic wave is less than 100 kHz,  $\lambda \approx 2000 \text{ m} \sim 3000 \text{ m}$ . Therefore, the frequency domain model of grounding system can be built without considering the electromagnetic wave process.

The frequency model of the grounding grid is established based on an integrated approach that combines Green's function of electric field and Kirchhoff current law of the circuit theory. It is assumed that there are  $n$  branches and  $m$  nodes in the grounding grid. For the square model, current is injected into the grounding grid, as shown in Fig. 1, where  $c$  is the end node of a conductor,  $d$  is the central node of a conductor.

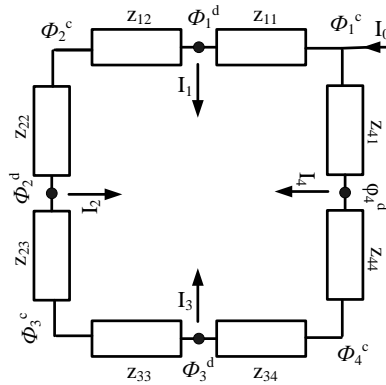


Fig. 1. Equivalent circuit diagram of a grounding grid.

Current dissipates into the ground while flowing along the conductors. Suppose the leakage current of the conductor flows into the ground from the central node of the conductor and the axial impedance is twice as high as the terminal impedance. The current dissipation would result in a voltage variation on the surface of all the conductors. In accordance with the Kirchhoff current law, the voltage equation for terminal nodes and central nodes would be:

$$\begin{bmatrix} B + R^{-1} & C \\ C^T & E \end{bmatrix} \begin{bmatrix} \phi^d \\ \phi^c \end{bmatrix} = \begin{bmatrix} 0 \\ I_0 \end{bmatrix}, \quad (2)$$

where  $\phi^d = [\phi_1^d, \phi_2^d, \dots, \phi_n^d]^T$ ,  $\phi_i^d$  is the central potential of conductor  $i$  ( $i = 1 \dots n$ );  $R$  is an  $n \times n$  matrix, i.e. the own impedance and the mutual impedance to ground;  $B$  is a

diagonal nonzero matrix, i.e. the own admittance of the central node of the conductor;  $C$  is a symmetric matrix, i.e. the mutual admittance between the central node and the terminal node for which the corresponding matrix element is zero if the nodes are connected;  $E$  is an  $m \times m$  matrix, i.e. the own impedance of the terminal nodes of the conductor;  $\phi^c = [\phi_1^c, \phi_2^c, \dots, \phi_n^c]^T$ ,  $\phi_i^c$  is the potential of node  $i$ ;  $I_0 = [I_0, 0, \dots, 0]^T$  is the injection current. Suppose  $I = [I_1, I_2, \dots, I_n]^T$ ,  $I_i$  is the leakage current of the conductor  $i$ . According to Green's function of the point current source, the relationship between the leakage current and the central potential can be expressed as follows:

$$I = R^{-1} \phi^d, \quad (3)$$

Therefore, all the leakage currents of the central nodes can be obtained. Suppose the coordinates of an arbitrary location  $Q$  on the surface are  $(x, y, z)$ , the surface potential of  $Q$  can be obtained by adding the potentials of all the leakage currents to  $Q$ .

## 2.2. Frequency characteristics of grounding conductors

When certain current flows in grounding conductors, the largest field lies in the surface of conductors and the internal field decreases gradually, known as Skin Effect, which is closely related to the Penetration Depth. It can be found through calculation that the Penetration Depth of the grounding conductors is much smaller than the penetration depth of soil under the effects of the steady electric field. So it is necessary to consider the Skin Effect of the grounding conductors as it will influence the distribution of leakage current. The own impedance of the conductor can be calculated as follows:

$$Z = \frac{1}{a} \sqrt{\frac{\mu f \rho}{2\pi}}, \quad (4)$$

where:  $\mu$  is the permeability of soil,  $a$  and  $\rho$  are the radius and the resistivity respectively,  $f$  is the frequency.

In the grounding grid, the axial current is observed flowing along grounding conductors and producing the mutual inductance between grounding conductors [15]. In order to simplify the calculation, grounding conductors are divided into micro sections of equal length. Assuming that each micro section is a linear current source, the formula for mutual inductive resistances is as follows:

$$M = l\rho \left( \ln \frac{2l}{d} - 1 \right) f, \quad (5)$$

where:  $l$  is length of the conductor,  $d$  is the distance between a couple of conductors,  $f$  is the frequency,  $\rho$  is the soil resistivity.

## 2.3. Frequency characteristics of soil

When varying frequencies are used to excite polarization in geophysics, it is found that the soil resistivity is changing in response to frequency change of the injection current. This may be explained by the excited polarization effect, which refers to the phenomenon that the additional electric field changes slowly due to electrochemical effects during the charge and discharge processes. According to the theory of equivalent circuit and polarization, the frequency dispersion model of soil resistivity is established [16]:

$$\rho(f) = \rho_0 \left[ 1 - \eta \left( 1 - \frac{1}{1 - 2\pi f \tau} \right) \right], \quad (6)$$

where:  $\rho_0$  is the resistivity for DC;  $\eta$  is the polarizable ratio, i.e.,  $\eta = (U_1 - U_2)/U_1$ ,  $U_1$  is the primary voltage,  $U_2$  is the secondary voltage;  $f$  is the frequency;  $\tau$  is the time constant.

Even when the frequency of the injection current is very low, the soil resistivity decreases with the increase of the injection current frequency. Environment conditions are set as follows: temperature 26°C, humidity 70%. A LCR4310 digital bridge produced by Wayne Kerr is used to test the frequency characteristic of clay soil (the material commonly found on the sites of substations), sand and water. It is found that the resistivity of soil and water gradually decreases with increasing frequency, as shown in Table 1.

Table 1. Frequency characteristic of the medium's resistivity.

NUMBER	1	2	3	4	5	6	7
Frequency [Hz]	30	50	100	1000	3000	5000	10000
Water resistivity [ $\Omega \cdot m$ ]	25.78	25.63	25.56	25.03	24.64	24.07	23.52
Sand resistivity [ $\Omega \cdot m$ ]	21.89	21.10	20.93	20.58	20.44	20.43	20.21
Clay soil resistivity [ $\Omega \cdot m$ ]	29.14	27.93	26.64	24.00	23.27	23.03	22.72

### 3. Fault diagnostic method of square-wave

When there is no fault, the topological structure of grounding grids remains unchanged after the substation is built. According to the uniqueness of the electric field, when the current flows along the grounding grid, the potential distribution is fixed above and under the substation. The metal conductors are easy to be corroded under certain circumstances. As a result of corrosion, part of the metal conductor becomes the oxides, whose frequency characteristics are similar to that of the soil. It has been found in the frequency model of the grounding system that the frequency characteristics of grounding conductors are different from those of soil medium around the grounding grid. When the metal conductors either completely or partly become oxides, which result in a fault of grounding grid, the topological structure of the grounding grid is altered. The leakage current changes and the surface potential of the grounding grid also changes. Therefore, by establishing the relation between the change of surface potential and the fault, the fault of the grounding grid can be diagnosed and located through the frequency-domain method.

In our method, a square-wave power supply is used instead of sinusoidal power supply for a number of reasons. For one thing, since the rise and decline of a square-wave are step signals, the Zero Crossing Point of a square-wave is extremely short, which is convenient for polarization. Moreover, the square-wave is a non-sinusoidal periodic component, which has many advantages such as the rapid rise time, the bipolar transform, etc. Through Fourier transform, the square-wave may be broken down into a series of sinusoidal signals of different frequencies, and excite responses at different resonant frequencies.

The grounding grid can be regarded as a black box system, which means the extent and location of corrosion are unknown. Through the injection of power sources of different frequencies, the surface potential of the grounding grid is acquired. And by analyzing and comparing the frequency characteristics of the surface potentials, the faults of the grounding grid can be detected and located.

## 4. Verification of the method

### 4.1 Simulation analysis

The diagnostic method of square-wave is verified by simulating and analyzing a complex 168 m × 188 m 220 kV substation grounding grid using Matlab. The soil structure is assumed to be uniform and of one layer. And the soil resistivity is set according to sand resistivity in Table 1. Horizontal grounding conductors are made of 150 mm<sup>2</sup> copper plated steel wires. Vertical grounding conductors are made of 158 mm<sup>2</sup> copper plated steel bars. The over-ground parts of the grounding-down-leads are made of 80 mm × 8 mm galvanized flat steel, and the below-ground parts of the grounding-down-leads are made of 185 mm<sup>2</sup> copper plated steel wire. The horizontal grounding grid is buried at the depth of 0.8 m. The 20 observation points selected are shown in Fig. 2.

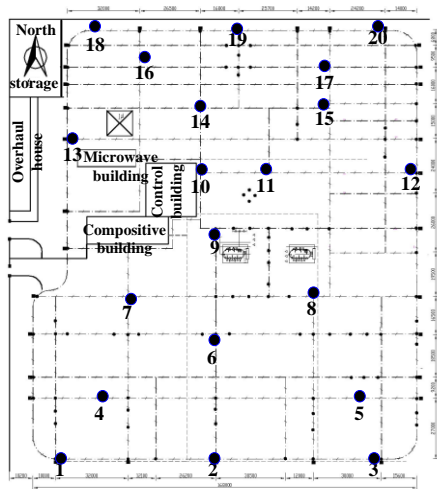


Fig. 2. Observation points of 220kV substation.

According to the frequency domain model of the grounding system, the surface potential caused by a square-wave of arbitrary frequency, which is injected into the grounding grid, can be calculated through Fourier inversion. Four fault cases are simulated and analyzed. As shown in Fig. 3, for example, the injection current is 3A, and the fault is placed between observation points 10 and 11, the surface potential differences are calculated.

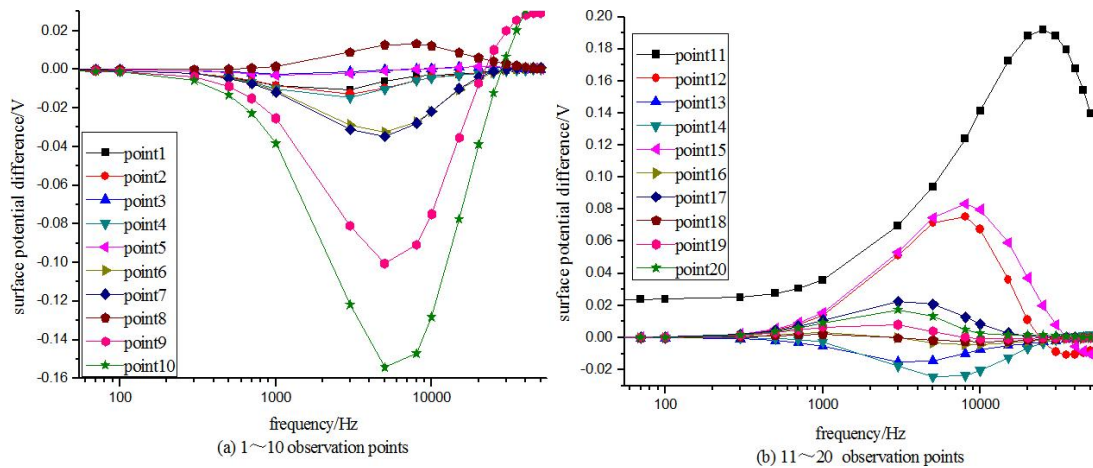


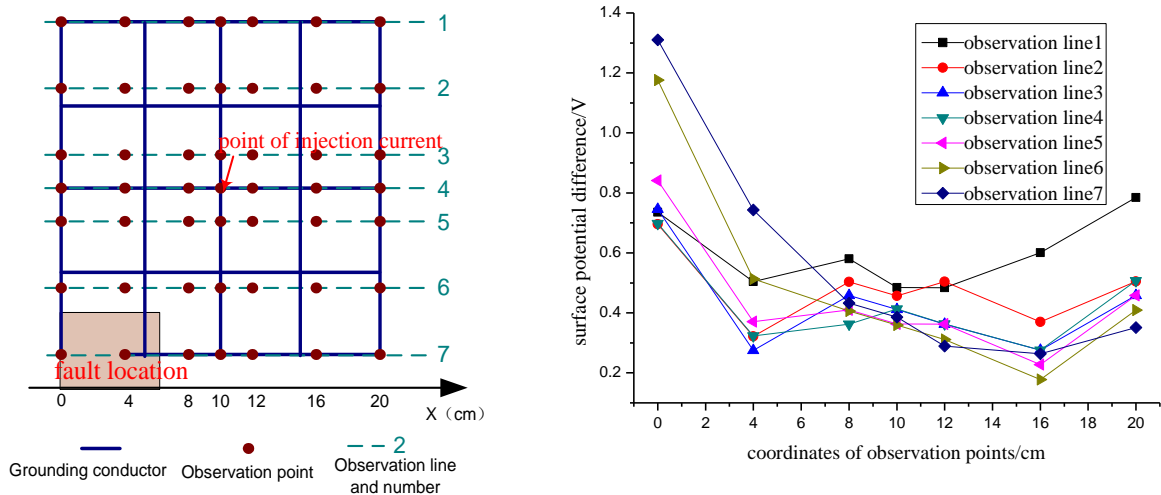
Fig. 3. Potential amplitude differences between observation points 1 ~20.

The surface potential of the observation point 10 ascends first and then descends along with the increase of frequency whereas that of the observation point 11 descends first and then ascends. Since the curves of observation points 10 and 11 deviate significantly from the other observation points, it may be inferred that the fault is located between observation points 10 and 11.

#### 4.2. Scale model experiment

The scale model experiments are conducted in a water tank based on the similarity theory. The geometric dimensions of the grounding grid, the buried depth, the current injecting grounding grid and the soil resistivity have been reduced. The dimension of the tank in the experiment is  $1.9\text{ m}\times 1.9\text{ m}\times 0.5\text{ m}$ , and the tank is filled with tap water as the medium. The distance between the model centre of the horizontal grounding grid and the wall of the tank is no less than five times the diagonal length of the model, which means the influence of diffused current on the wall is negligible. In order to simulate the Zero Potential of the actual surface of the grounding grid, the four sides and the bottom of the tank are covered with a layer of iron sheet connected to the ground, and the grounding grid has been laid in the centre of the tank. Medical needles with a diameter of 0.25 mm have been used as the measuring probes of surface potential. The immersed parts of probes in water have been wrapped by heat shrinkable tube in order to avoid distortion of the electric field. Frequency adjustable (between 30 Hz~10 kHz) sinusoidal current and square-wave current have been designed.

Multiple fault experiments are conducted on different grounding grids. For example, a  $20\text{ cm}\times 20\text{ cm}$  grounding grid has been placed 5 cm underneath the water. The depth of the potential probe is 1 cm. 7 observation lines for surface potential are selected and 7 observation points from 1~7 are selected on each observation line. A fault has been placed on the edge of the grounding grid. The observation points on the grounding grid and the measurement results are shown in Fig. 4.



a) observation points for surface potential

b) surface potential differences at different observation points

Fig. 4. Observation points and surface potential difference (3 kHz).

Fig. 4 shows that the largest differences of surface potential are observed between observation points 2 and 4 on the observation line 7, which is the location of the fault. The experimental results show that the fault can be detected and the location of the fault can be identified.

### 4.3. Field experiments

Subsequently, field experiments have been conducted in which square-wave diagnosis apparatus of the grid fault has been used. The grounding grid of a 16 m × 20 m high-voltage experimental hall is taken as the main grid of the experiment, and an assistant grid consisting of five 5 mm × 50 mm × 5 m steel flats is buried at a depth of 0.5 m. A steel rod with the diameter of 2 cm and the length of 1 m are welded to the middle of the steel flat as the vertical grounding down-lead. 10 observation points have been selected as shown in Fig. 5. Metal disks with the diameter of 20 cm and the weight of 1.5 kg are used as the potential measuring electrodes, wrapped by wet sponge in order to make contact with the ground. Special iron rods with length of 530 mm are used as the electrodes for current injection.

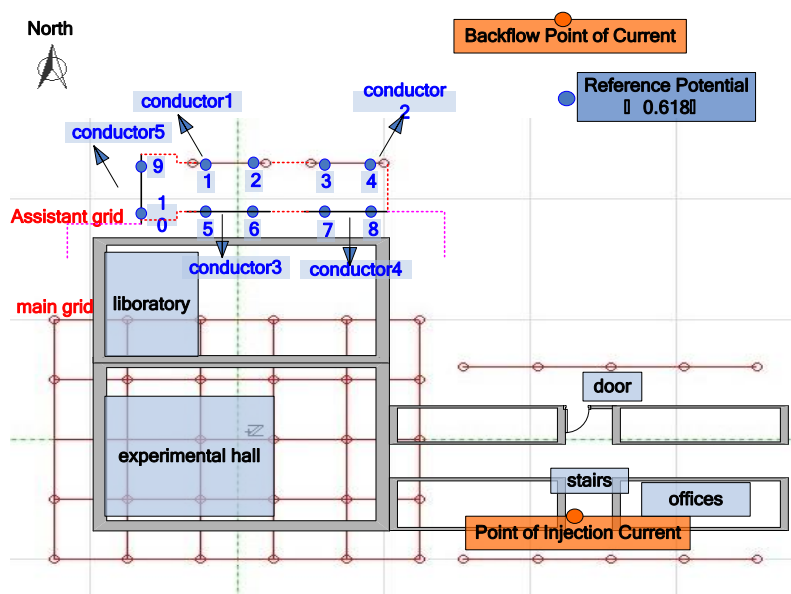


Fig. 5. Observation points of a factual grounding grid.

Three experimental schemes have been designed to simulate the two faults through the combination of opening or closing switches:

Scheme I: All 5 conductors (conductors 1 to 5) connect to the main grid according to the dotted line shown in Fig. 5.

Scheme II: All 5 conductors except conductor 3 connect to the main grid.

Scheme III: only conductors 1, 2 and 5 connect to the main grid.

Because the area of the grounding grid is usually large, the power of the current sources injected into the grounding grid would be much larger. Since it is difficult to manufacture such a large current source of varying frequencies, two current sources are injected into the grounding grid. If the frequency is too low, it would be interfered by the ground current largely; on the contrary, if the frequency is too high, it would be interfered by the electromagnetic coupling between the power supply and the measurement circuit. Therefore, 50 Hz AC and 3 kHz square-wave are selected. They are injected into the grounding grid according to the three schemes respectively. In order to avoid on-site interference of the power frequency of 50 Hz AC, the mean value of surface potentials produced by a 55 Hz AC current and a 45 Hz AC current has been used as the surface potential of a 50 Hz AC current. The backflow point of current is selected 100 meters far from the lab. The surface potentials observed are shown in Fig. 6.

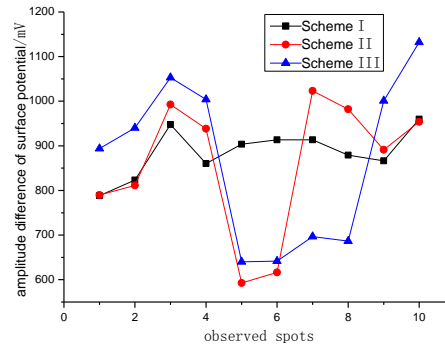


Fig. 6. Comparison results of different frequencies.

In Fig. 6, the surface potential differences of points 5 and 6 above conductor 3 in Scheme II are evidently smaller than the differences above other conductors, because conductor 3 is not connected to the main grounding grid in Scheme II. It is similar in Scheme III that the differences of points from 5 to 8 above conductors 3 and 4 in Scheme III are obviously smaller than the surface potential difference above other conductors, because conductors 3 and 4 are not connected to the main grounding grid in Scheme III. The results suggest that the grid fault can be correctly diagnosed using a square-wave of different frequencies. It is also reasonable to suggest that our method can be applied to diagnose and locate faults in real substations. Although the grounding grid of the real substations is more complicated, its environmental condition and the geological condition are similar. When the local corrosion causes a fault, the length of corrupted grounding conductors is usually of a few meters. Therefore, if the injection current is fixed, the surface potential in fault location is reduced. Therefore, by monitoring the changes of surface potential, faults in the grounding grid can be diagnosed and located. Potential-measuring electrodes are usually arranged with definite interval order (for example, 10 m) inside the substation, according to the buried direction of horizontal grounding conductors. After measuring and recording the surface potential of each point, the data mining algorithm may be applied to find the special points which indicate whether the substation grounding grid is corroded or not, and the corrosive position if it had been corroded.

## 5. Conclusions

In this study, a frequency model of the grounding system is presented by analyzing the frequency characteristics of the soil and the grounding conductors. A fault diagnostic method of the grounding grid using a square-wave is proposed based on the frequency model of the grounding system. The faults of the grounding grid are detected and located by analyzing and comparing the surface potentials of different frequency. Software simulation of the substation grounding grid, scale model experiments of small dimension and field experiments of complicated structure are conducted to verify the method. The results suggest that the method can be used to diagnose faults effectively and locate them accurately without excavating the grounding grids.

## Acknowledgement

Mr. Ho Simon Wang at HUST Academic Writing Centre has helped improve the presentation of the manuscript.

## References

- [1] Zhang, Xiuli, Luo, Ping, Mo, Ni. (2008). Development and application of electrochemical detection system for grounding grid corrosion state. *Proceedings of the CSEE*, 28(19), 152-156.
- [2] Liu, Jian, Wang, Jianxin, Cheng, Hongli. (2006). Data mining in grounding grid corrosion detection to ensure safety of electric power systems. *Proceedings of the 2006 International Symposium on Safety Science and Technology*, Changsha, China, 472-478.
- [3] Rong, Zeng, Jinliang, He, Jun, Hu. (2002). The theory and implementation of corrosion diagnosis for grounding system. *International Conference on Power System Technology*, Pittsburgh, USA, 1120-1126.
- [4] Wilen, T. (2003). Electrical grounding systems & testing. *Michigan Tech.*, 11, 1-20.
- [5] Grcev, L, Dawalibi, F. (1990). An electromagnetic model for transients in grounding systems. *IEEE Transaction on Power Delivery*, 5(4), 1773-1781.
- [6] Tsuchida, T., Tsuneoka, M., Ohkawa, Y., et al. (2008). Basic study of high-frequency impedance characteristics of ground system. *IEEE Trans on Industry Applications*, 128(11), 1239-1246.
- [7] Cidras, J., Tero, A.F., Carrido, C. (2000). Nodal frequency analysis of grounding systems considering the soil ionization effect. *IEEE Transactions on Power Delivery*, 15(1), 1083-1091.
- [8] Wlater, J.M. (2006). Ground resistivity influence on the lightning over-voltage level in high voltage power substation [C]. *XVI international conference on electromagnetic disturbances*, Kaunas.
- [9] Liu, Yang, Cui, Xiang, Zhao, Zhibin. (2008). Design and application of exciting power for substation grounding grids testing system based on impedance transformation technology. *Proceedings of the CSEE*, 28(28), 18-23.
- [10] Hsu, Ting-Yu, Loh. (2009). Damage detection using frequency response functions under ground excitation. *Proceedings of SPIE - The International Society for Optical Engineering*, 7292(1), 65-71.
- [11] Jordan, J., Gasulla, M., Pallas-Areny, R. (2001). Electrical resistance tomography to detect leaks from buried pipes. *Measurement Science and Technology*, 12, 1061-1070.
- [12] Ksiazek, M. (2011). The experimental and innovative research on usability of sulphur polymer composite for corrosion protection of reinforcing steel and concrete. *Composites Part B: Engineering*, 42(5), 1084-1096.
- [13] Donze, T. (2006). Electromagnetic survey defines reservoir, prevents drilling poor prospect. *World Oil*, 224(5), 85-87.
- [14] Rosendo, V.B., Harneit, S., Reuter, M. (2006). Moisture effects in soils using a frequency domain metal detector. *2006 World Automation Congress*, 6, 21-26.
- [15] Lee Kyeong-Hwan, Zhang Naiqian, Kuhn William B, et al. (2007). A frequency-response permittivity sensor for simultaneous measurement of multiple soil properties: Part I. The frequency-response method. *Transactions of the ASABE*, 50(6): 2315-2326.
- [16] Huang, Wenwu, Wen, Xishan, Xie, Jun. (2005). Simulation of the current distribution along axial direction of the grounding network. *High Voltage Engineering*, 31(6), 76-78.